PROCEEDINGS OF SCIENCE

Exclusive heavy vector meson photoproduction with momentum transfer squared dependence in UPCs

Cheryl Henkels[a,*]

[a] *Departamento de Física, CFM, Universidade Federal de Santa Catarina, C.P. 476, CEP 88.040-900, Florianópolis, SC, Brazil*

E-mail: cherylhenkels@hotmail.com

The exclusive photoproduction of the heavy vector mesons $\psi(1S)$, $\psi(2S)$, $\Upsilon(1S)$ and $\Upsilon(2S)$ is studied using the b-BK and the "bSat" dipole models with a vector meson wave function obtained by a potential approach incorporating the Melosh spin rotation. The results for the proton-target scattering agreed with the HERA data. For the nuclear case, we extended our calculations with the Glauber-Gribov theory and we included the gluon shadowing effects with a nuclear PDF. The results were compared to the ALICE data for the J/ψ photoproduction at $s_{NN} = 5.02$ TeV.

XV International Workshop on Hadron Physics (XV Hadron Physics) 13 -17 September 2021
Online, hosted by Instituto Tecnológico de Aeronáutica, São José dos Campos, Brazil

*Speaker

PoS(XVHadronPhysics)021

1. Introduction

One of the major interests of particle physics is the understanding of the structure of protons and nuclei regarding their fundamental constituents and interactions [1]. Differential observables can be seen as an effective tool to obtain a more detailed picture of the target's internal structure. In the literature, the Deeply Virtual Compton Scattering (DVCS) and the exclusive vector meson photoproduction are the two most discussed processes that give differential observables. In the past, the high beam energy of the HERA collider permitted that the experiments H1 and ZEUS measured the pure DVCS cross section from $x_B = 10^{-4}$ to $x_B = 10^{-2}$. However, in the vector meson photoproduction case, in addition to the H1 and ZEUS measurements (for ϕ, ρ, and J/ψ), some newer data were obtained in ultraperipheral collisions by the LHC collaboration [2–6].

One advantage of study the vector meson production is that, in order to produce only the vector meson and nothing else, a color charge cannot be transferred to the target, requiring that at least two gluons need to be exchanged. In the dipole model, it is considered that these gluons are exchanged between a $q\bar{q}$ pair, generated by a photon split, and the target. This is typically validated by a hard scale, which is associated with the heavy-quark mass. Thus, heavy vector mesons such as $\Upsilon(1S)$ and $\Upsilon(2S)$ provide a sufficiently hard scale (m_b) for the application of perturbative calculations, while the production of not so heavy mesons such as $\psi(1S)$ and $\psi(2S)$ presents a semi-hard scale (m_c), which can lead to the appearance of non-perturbative effects. Hence, finding a formalism capable of describing the data for both vector mesons is a good way to test the efficiency of the parameterizations responsible to take into account the non-perturbative part of the interaction and validate the universality of the formalism.

The dipole-target interaction is often parameterized by a Gaussian distribution that contains saturation effects, this is the case of the very known "bSat" model. An alternative description to obtain the amplitude of this interaction is by solving the Balitsky-Kovchegov (BK) equation. It is known that the full NLO-BK equation is unstable because of the large and negative NLO corrections that comes from integrating out gluon emissions with small transverse momenta, so these corrections need to be properly resummed to all orders [7]. Besides this, when the impact parameter dependence is added, a phenomenon called Coulomb tails appears [8] (an unphysical grow of the amplitude at large impact parameters), which is found to be linked to the fact that the kernel suppresses large daughter dipoles. Solutions without this Coulomb tails can be found in some papers such as [9, 10]. In this work, we used both the "bSat" and BK solution models within the dipole formalism to calculate the differential cross sections for the vector meson photoproduction and we used a potential approach based on solving the Schroedinger equation to obtain the vector meson wave functions along with the Melosh spin rotation.

2. Photoproduction off a proton target

The interaction between the photon and the proton can be described by the dipole model, which is based on the fact that on quantum mechanics the photon can fluctuate in a $q\bar{q}$ pair, which can strongly interact with the proton. This approach is valid because in the proton rest frame, the fluctuation lifetime is bigger than the interaction time of the $q\bar{q}$ pair with the proton, which makes it possible to separate the process into three steps. First, the photon splits into a $q\bar{q}$ pair (the color

dipole), then this dipole interacts strongly with the proton, by an exchange of gluons, and finally the recombination of the $q\bar{q}$ pair into a vector meson takes place.

The scattering amplitude of this process is given by the product of the amplitude of each subprocess integrated in β and r, which are the momentum fraction carried by the quark and the transverse separation of the $q\bar{q}$ pair, respectively.

$$\mathcal{A}^{\gamma p}(x, \Delta_T) = \int \mathrm{d}^2\boldsymbol{r} \int_0^1 \mathrm{d}\beta \psi_V^*(r,\beta)\psi_\gamma(r,\beta)\mathcal{A}_{q\bar{q}}(x, \boldsymbol{r}, \boldsymbol{\Delta}) \,. \tag{1}$$

As you can see, in the equation, ψ_γ is the photon wave function, ψ_V is the vector meson wave function and $\Delta_T \equiv |\boldsymbol{\Delta}|$ is the transverse momentum of the produced vector meson.

In our previous works [11, 12], we chose to use a vector meson wave function obtained by first principles. Thus, following the same potential approach [13, 14], we factorized the wave function into a spin-dependent part and a spatial one. The spatial part of the wave function is obtained by solving the non-relativistic Schroedinger equation for heavy quark interaction potentials in the dipole rest frame. However, since we want to substitute it on the forward amplitude (Eq. 1), a Lorentz transformation needs to be applied to ψ_V to boost it to the infinite momentum frame, where the dipole model is defined. In this analysis, we used five different models for the $q\bar{q}$ interaction potential: power-like model [15, 16] (pow), harmonic oscillator (osc), Cornell potential [17, 18] (cor), Buchmüller-Tye parametrisation [19] (but) and logarithmic potential [20] (log). These models' parameters were fitted to the hadron spectrum, thus we assured to use the same ones, as in the original fits, when solving the Schroedinger equation, including the heavy quark masses.

It is important to emphasize that when fitting the interquark potentials, the quark masses obtained are not bare masses, since they have non-perturbative effects that are different for each potential, thus they are allowed to vary in order to improve the potential parameterization. To keep the universality of the color dipole model, we chose to employ fixed perturbative masses on the scattering amplitude, which are $m_c = 1.4$ GeV for charm quarks and $m_b = 4.75$ GeV for bottom quarks.

The Lorentz transformation between the two frames requires a boost not only on the radial part but also on the spin-dependent part of the wave function. Such transformation that takes the quark spinors from the $q\bar{q}$ rest frame to the infinite momentum frame, is known as the Melosh spin rotation [21]. This has a significant effect on differential photoproduction cross sections, particularly for excited quarkonia states [13, 22].

The last ingredient in Eq. 1 to be explained is $A_{q\bar{q}}$, which represents the elementary elastic amplitude of the interaction of the dipole with the proton. The optical theorem permits us to rewrite this elementary elastic amplitude $A_{q\bar{q}}$ in terms of the partial dipole amplitude $N(x, r, b)$, which is defined as the imaginary part of the former. Thus, the non-forward amplitude of the photon-proton scattering is given by [23]:

$$\mathcal{A}^{\gamma p}(x, \Delta_T) = 2i \int \mathrm{d}^2\boldsymbol{r} \int_0^1 \mathrm{d}\beta \int \mathrm{d}^2\boldsymbol{b} \psi_V^*(r,\beta)\psi_\gamma(r,\beta)\mathrm{e}^{-i[\boldsymbol{b}-(1-\beta)\boldsymbol{r}]\cdot\boldsymbol{\Delta}} N(x, \boldsymbol{r}, \boldsymbol{b}) \,. \tag{2}$$

Since the partial dipole amplitude includes corrections related to gluon radiations, it cannot be calculated with pQCD, so phenomenological parameterizations are employed to describe it. For the main purpose of calculating t differential cross section, we used two different b-dependent

elementary elastic amplitude models: the impact parameter dipole saturation model [23] (known as "bSat") and the model based upon a numerical solution of the Balitsky-Kovchegov (BK) equation [9].

Another consequence of the use of the optical theorem is that it makes necessary the inclusion of two correction terms. One to account for the real part of the amplitude [14], which is given by the following substitution:

$$\mathcal{A}^{\gamma p} \Rightarrow \mathcal{A}^{\gamma p}\left(1 - i\frac{\pi\lambda}{2}\right), \quad \text{with} \quad \lambda = \frac{\partial \ln \mathcal{A}^{\gamma p}}{\partial \ln(1/x)}, \tag{3}$$

and the other to consider the skewness effect, which comes from the fact that the two gluons exchanged between the $q\bar{q}$ pair and the nucleon can carry different momentum fractions. This effect is included by the multiplication of the scattering amplitude by the factor [24]:

$$R_g(\lambda) = \frac{2^{2\lambda+3}}{\sqrt{\pi}} \frac{\Gamma(\lambda + 5/2)}{\Gamma(\lambda + 4)}. \tag{4}$$

With all the amplitude's ingredients defined, it is possible to calculate the elastic differential cross-section in t for the $\gamma p \to Vp$ scattering, which is defined as [23, 25]:

$$\frac{\mathrm{d}\sigma^{\gamma p \to Vp}}{\mathrm{d}t} = \frac{1}{16\pi} \left|\mathcal{A}^{\gamma p}(x, \Delta_T)\right|^2. \tag{5}$$

This equation is the essential basic key for the description of the actually available HERA data and the future measurements that can be realized by LHC and EIC.

2.1 Results for ψ and Υ photoproduction

The Fig. 1 shows the results of the differential cross-section as a function of the transferred momentum t for both the photoproduction of ψ states at a center of mass energy of 100 GeV. On the left panel, the results for $\psi(1S)$ (upper curves) and $\psi(2S)$ (lower curves) were obtained using a numerical solution of the BK equation [9] and five different parameterizations of the interquark potential [15, 18–20]. Since the differential photoproduction cross sections are, in general, sensitive to the partial dipole amplitude parameterization, we chose to show (on the right panel) the $\psi(1S)$ results calculated with two different models: one obtained by the solution of the BK equation (explained above) and other the very known saturation model "bSat" [23]. In order to do this comparison, we chose the wave function calculated with Buchmüller-Tye potential, which was not a special choice because, as can be seen on the left panel, the differences between the $\psi(1S)$ differential cross sections calculated with different potentials are practically imperceptible. A comparison between the $\psi(1S)$ results with the corresponding data from H1 Collaboration [26, 27] revealed that the BK model describes better the H1 data that the bSat one. Furthermore, some predictions for the differential cross section of $\Upsilon(1S)$ (left) and $\Upsilon(2S)$ (right) photoproduction are presented in Fig. 2 as a function of $|t|$, also using the BK equation numerical solution, for $W = 120$ GeV. These positive results for the proton target were important to verify the formalism and encouraged us to extend them to the nuclear target case.

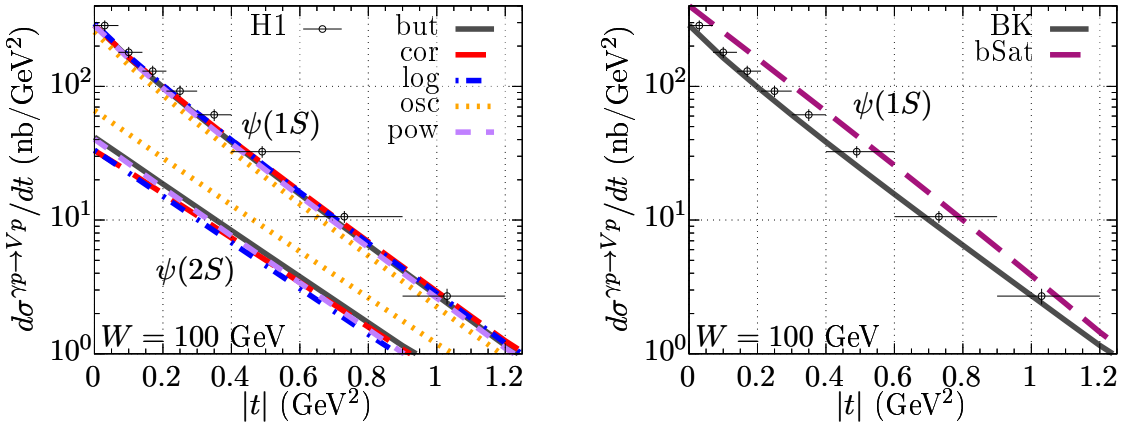

Figure 1: Differential cross section for $\psi(nS)$ photoproduction as a function of $|t|$ for $W = 100$ GeV. On the left panel, the results for $\psi(1S)$ (upper curves) and $\psi(2S)$ (lower curves) are calculated with the numerical solution of the BK equation obtained in Ref. [9], using five different interquark potential models [15, 18–20]. In order to compare different dipole models, on the right panel the $\psi(1S)$ cross section is calculated just with the Buchmüller-Tye potential, however with both the BK and the "bSat" model [23]. In both panels the $\psi(1S)$ results are compared to the corresponding data from H1 Collaboration [26, 27].

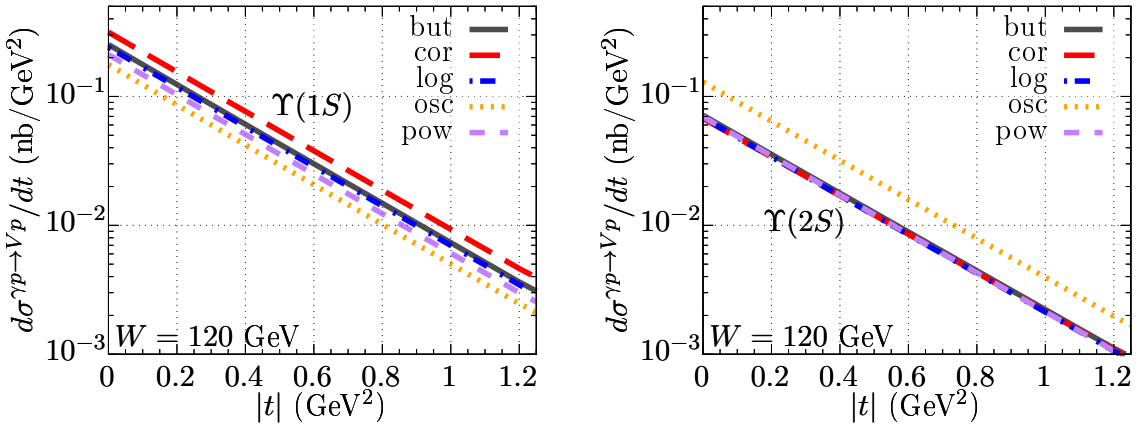

Figure 2: Predictions for the differential cross section for $\Upsilon(1S)$ (left) and $\Upsilon(2S)$ (right) as a function of $|t|$ obtained using the BK numerical solution, for $W = 120$ GeV. The results are presented for five different interquark potential models.

3. Photoproduction off a nuclear target

In processes where the target is a nucleus, the vector meson can be produced coherently, which means that the nucleus target will remain intact after the collision. In this case, the differential cross-section is proportional to the square of the averaged photon-nucleus amplitude. Since this average is taken over all possible configurations of the nucleons inside the nucleus, it is an interesting tool to study the average shape of the target.

$$\frac{\mathrm{d}\sigma^{\gamma A\to VA}}{\mathrm{d}t} = \frac{1}{16\pi}\left|\left\langle \mathcal{A}^{\gamma A\to VA}(x,\Delta)\right\rangle\right|^2 . \tag{6}$$

In the dipole model at high energies, the lifetime of the $q\bar{q}$ pair is larger than the nuclear radius.

This guarantees a small variation of the transverse size of the dipole system and no fluctuations during the propagation through the nucleus. Thus, we can use the Glauber-Gribov model to calculate the average of the photon-proton amplitude [12],

$$\begin{aligned}\left\langle \mathcal{A}^{\gamma A\to VA}(x,\Delta)\right\rangle =& i\int \mathrm{d}^2\mathbf{r}\int_0^1 \mathrm{d}\beta\int \mathrm{d}^2\mathbf{b}\, e^{-i[\mathbf{b}-(1-z)\mathbf{r}]\cdot\mathbf{\Delta}}\\ &\times \Sigma_T(r,\beta)\, 2\left[1-\exp\left(-\frac{AT_A(b)\sigma_{q\bar{q}}(x,r)}{2}\right)\right],\end{aligned} \tag{7}$$

which $\Sigma_T = \Sigma^{(1)} + \Sigma^{(2)}\frac{\mathrm{d}}{\mathrm{d}r}$ represents the overlap between the photon and the vector meson wave functions including the Melosh spin rotation (the expressions for $\Sigma^{(1)}$ and $\Sigma^{(2)}$ can be found on our previous papers [11, 12]). This expression is very similar to the proton-target one, however, instead of the partial dipole amplitude, inside the brackets, there is an expression proportional to the nuclear thickness function $T_A(b)$ and the total dipole-proton cross section $\sigma_{q\bar{q}}$, which is given by:

$$\sigma_{q\bar{q}}(x,r) = 2\int \mathrm{d}^2\boldsymbol{b}\, N(x,\boldsymbol{r},\boldsymbol{b})\,. \tag{8}$$

In the high energy limit, one has to consider that the gluon density inside the nucleus is smaller than the one for free nucleons. The name of this effect is gluon shadowing and it can be taken into account by renormalizing the dipole cross section,

$$\sigma_{q\bar{q}}(r,x) \to \sigma_{q\bar{q}}(r,x)R_G(x,\mu^2)\,. \tag{9}$$

In this equation, the factor R_G is given by the ratio between the gluon density inside a nucleus' nucleon and the one found in a free nucleon

$$R_G(x,\mu^2) = \frac{xg_A(x,\mu^2)}{Axg_p(x,\mu^2)}\,. \tag{10}$$

In this paper we chose to use the nuclear parton distribution function (PDF) EPPS16 [28] and the proton PDF CT14 [29] for the evaluation of this factor.

3.1 Results for ψ and Υ photoproduction

The formalism presented above permitted us to calculate the differential cross section of the vector meson coherent photoproduction in γA collisions. The vector meson wave functions were obtained by the potential approach, however, since the differences between the results obtained with different potentials were practically unnoticed, we chose to show only the curves obtained with the Buchmüller-Tye potential [19]. For the total dipole-proton cross section we chose to make a comparison between three dipole models: the numerical solution of the BK equation, the bSat model, and also the phenomenological GBW model [30]. Furthermore, the effects of the gluon shadowing were included by renormalizing the dipole cross-section by a factor calculated fully phenomenologically with PDFs [28, 29].

In Fig. 3 we show a comparison between the results for the $\psi(1S)$ differential cross section and the ALICE data [3] at $\sqrt{s} = 5.02$ TeV. We found that the curves underestimate the $\psi(1S)$ data for

photoproduction at small $|t|$, and that the bSat model performed better than the others in describing the data. We also present predictions for the differential cross section for the $\psi(2S)$ photoproduction at the same energy. Additionally, with the expectation that the future colliders could make some measurements at larger t values, we produced some predictions for the differential cross section of the $\gamma Pb \to VPb$ coherent ψ (left panel) and Υ (right panel) photoproduction at $\sqrt{s} = 5.02$ TeV for a large range of $|t|$, and show them in Fig. 4.

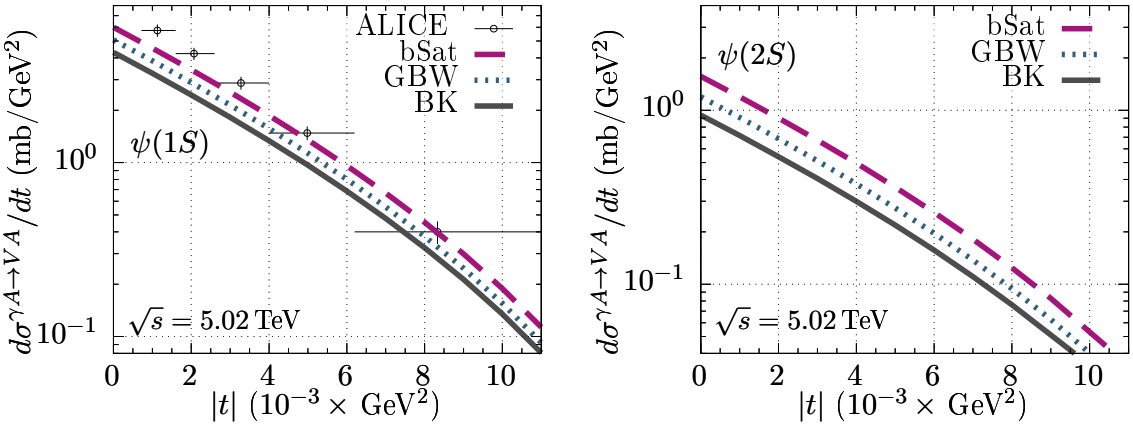

Figure 3: Differential cross sections for the $\gamma Pb \to \psi(nS)Pb$ process as functions of $|t|$, with wavefunctions calculated using the Buchmüller-Tye potential. In the $\psi(1S)$ case (left panel), the results using the BK and bSat dipole amplitudes and the purely phenomenological GBW dipole cross section [30] are compared with the ALICE data for $\sqrt{s} = 5.02$ TeV [3].

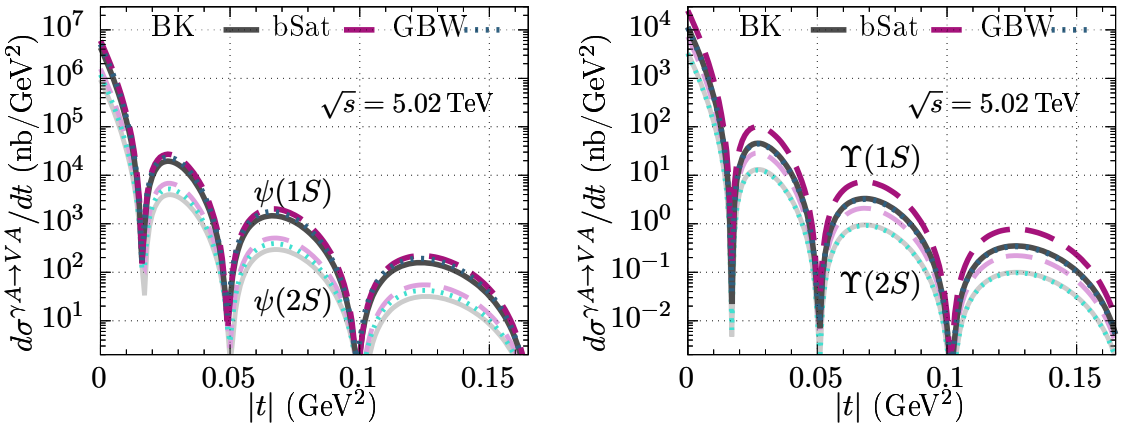

Figure 4: Predictions for the differential cross sections for the $\gamma Pb \to VPb$ processes as functions of $|t|$, calculated with three dipole cross section models: the numerical solution of the BK equation for the dipole amplitude, the bSat model and the GBW parameterisation. The results are shown for the production of ψ states (left) and Υ states (right). Both panels present the results at $y = 0$ and with $\sqrt{s} = 5.02$ TeV.

4. Conclusion

In this work, we studied the exclusive photoproduction of the vector mesons $\psi(1S)$, $\psi(2S)$, $\Upsilon(1S)$ and $\Upsilon(2S)$ with proton and nuclear targets within the dipole formalism. An essential part of

this formalism is the vector meson wave function, which in this work was obtained by a potential approach, that consists in solving the Schroedinger equation on the $q\bar{q}$ rest frame with different interquark potentials and boost it to the infinite momentum frame, with the inclusion of the Melosh spin rotation. This enables the calculation of the differential cross section in t for both the ground and excited states of the charmonium and the bottomonium.

Furthermore, on the dipole-proton interaction amplitude we used two models to describe the H1 Collaboration available data [26, 27] for the J/ψ photoproduction: the bSat and BK models. The results obtained with the inclusion of the real part of the scattering amplitude and the skewness effect in the scattering amplitude at the γp level showed that the BK model provided a better description of the available data in the proton target case. This setup also make it possible to make predictions for the mesons $\psi(2S)$, $\Upsilon(1S)$ and $\Upsilon(2S)$.

For the nuclear case, we used the Glauber-Gribov approach for high energy scatterings and included the gluon shadowing phenomenologically with a nuclear PDF to describe the photon-nucleus interaction. The results calculated with the Buchmüller-Tye vector meson wave function were compared with the ALICE data [3] and showed that the bSat model described more accurately this data than the other models. This shows that the existing parameterizations for the partial dipole amplitude still contain significant uncertainties. With this setup, we also presented predictions for all four vector mesons in a larger t range with the hope that someday this quantities will be measured on the LHC or on other future coliders, like the FCC or the EIC [31].

Acknowledgments

CH would like to thank the collaborators Emmanuel G. de Oliveira, Haimon Trebien and Roman Pasechnik for their important contributions to this project. This work was supported by Fapesc, INCT-FNA (464898/2014-5), and CNPq (Brazil). This study was financed by the Coordenação de Aperfeiçoamento de Pessoal de Nível Superior – Brasil (CAPES) – Finance Code 001.

References

[1] H. Mäntysaari, *Review of proton and nuclear shape fluctuations at high energy*, *Rept. Prog. Phys.* **83** (2020) 082201 [2001.10705].

[2] V. Gonçalves, F. Navarra and D. Spiering, *Exclusive ρ and J/Ψ photoproduction in ultraperipheral pA collisions: Predictions of the gluon saturation models for the momentum transfer distributions*, *Phys. Lett. B* **791** (2019) 299 [1811.09124].

[3] ALICE collaboration, *First measurement of the $|t|$-dependence of coherent J/ψ photonuclear production*, *Phys. Lett. B* **817** (2021) 136280 [2101.04623].

[4] CMS collaboration, *Measurement of exclusive Υ photoproduction from protons in pPb collisions at $\sqrt{s_{NN}} = 5.02$ TeV*, *Eur. Phys. J. C* **79** (2019) 277 [1809.11080].

[5] ALICE collaboration, *Coherent photoproduction of ρ^0 vector mesons in ultra-peripheral Pb-Pb collisions at $\sqrt{s_{NN}} = 5.02$ TeV*, *JHEP* **06** (2020) [2002.10897].

[6] ALICE collaboration, *First measurement of coherent ρ0 photoproduction in ultra-peripheral Xe–Xe collisions at sNN=5.44 TeV*, *Phys. Lett. B* **820** (2021) 136481 [2101.02581].

[7] B. Ducloué, E. Iancu, G. Soyez and D.N. Triantafyllopoulos, *HERA data and collinearly-improved BK dynamics*, *Phys. Lett.* **B803** (2020) 135305 [1912.09196].

[8] K.J. Golec-Biernat and A.M. Stasto, *On solutions of the Balitsky-Kovchegov equation with impact parameter*, *Nucl. Phys. B* **668** (2003) 345 [hep-ph/0306279].

[9] D. Bendova, J. Cepila, J.G. Contreras and M. Matas, *Solution to the Balitsky-Kovchegov equation with the collinearly improved kernel including impact-parameter dependence*, *Phys. Rev.* **D100** (2019) 054015 [1907.12123].

[10] J. Cepila, J.G. Contreras and M. Matas, *Predictions for nuclear structure functions from the impact-parameter dependent Balitsky-Kovchegov equation*, 2002.11056.

[11] C. Henkels, E.G. de Oliveira, R. Pasechnik and H. Trebien, *Exclusive photoproduction of excited quarkonia in ultraperipheral collisions*, *Phys. Rev. D* **102** (2020) 014024 [2004.00607].

[12] C. Henkels, E.G. de Oliveira, R. Pasechnik and H. Trebien, *Momentum transfer squared dependence of exclusive quarkonia photoproduction in ultraperipheral collisions*, *Phys. Rev. D* **104** (2021) 054008 [2009.14158].

[13] J. Cepila, J. Nemchik, M. Krelina and R. Pasechnik, *Theoretical uncertainties in exclusive electroproduction of S-wave heavy quarkonia*, *Eur. Phys. J. C* **79** (2019) 495 [1901.02664].

[14] J. Hufner, Y.P. Ivanov, B.Z. Kopeliovich and A.V. Tarasov, *Photoproduction of charmonia and total charmonium proton cross-sections*, *Phys. Rev.* **D62** (2000) 094022 [hep-ph/0007111].

[15] A. Martin, *A FIT of Upsilon and Charmonium Spectra*, *Phys. Lett.* **93B** (1980) 338.

[16] N. Barik and S.N. Jena, *FINE - HYPERFINE SPLITTINGS OF QUARKONIUM LEVELS IN AN EFFECTIVE POWER LAW POTENTIAL*, *Phys. Lett.* **97B** (1980) 265.

[17] E. Eichten, K. Gottfried, T. Kinoshita, K.D. Lane and T.-M. Yan, *Charmonium: The Model*, *Phys. Rev.* **D17** (1978) 3090.

[18] E. Eichten, K. Gottfried, T. Kinoshita, K.D. Lane and T.-M. Yan, *Charmonium: Comparison with Experiment*, *Phys. Rev.* **D21** (1980) 203.

[19] W. Buchmuller and S.H.H. Tye, *Quarkonia and Quantum Chromodynamics*, *Phys. Rev.* **D24** (1981) 132.

[20] C. Quigg and J.L. Rosner, *Quarkonium Level Spacings*, *Phys. Lett.* **71B** (1977) 153.

[21] H.J. Melosh, *Quarks: Currents and constituents*, *Phys. Rev.* **D9** (1974) 1095.

[22] M. Krelina, J. Nemchik, R. Pasechnik and J. Cepila, *Spin rotation effects in diffractive electroproduction of heavy quarkonia*, *Eur. Phys. J.* **C79** (2019) 154 [1812.03001].

[23] H. Kowalski, L. Motyka and G. Watt, *Exclusive diffractive processes at HERA within the dipole picture*, *Phys. Rev.* **D74** (2006) 074016 [hep-ph/0606272].

[24] A. Shuvaev, K.J. Golec-Biernat, A.D. Martin and M. Ryskin, *Off diagonal distributions fixed by diagonal partons at small x and xi*, *Phys. Rev. D* **60** (1999) 014015 [hep-ph/9902410].

[25] J.R. Forshaw and D.A. Ross, *Diffraction*, Cambridge Lecture Notes in Physics, Cambridge University Press, Cambridge (1997), 10.1017/CBO9780511524387.008.

[26] H1 collaboration, *Elastic and Proton-Dissociative Photoproduction of J/psi Mesons at HERA*, *Eur. Phys. J. C* **73** (2013) 2466 [1304.5162].

[27] H1 collaboration, *Elastic J/psi production at HERA*, *Eur. Phys. J.* **C46** (2006) 585 [hep-ex/0510016].

[28] K.J. Eskola, P. Paakkinen, H. Paukkunen and C.A. Salgado, *EPPS16: Nuclear parton distributions with LHC data*, *Eur. Phys. J.* **C77** (2017) 163 [1612.05741].

[29] S. Dulat, T.-J. Hou, J. Gao, M. Guzzi, J. Huston, P. Nadolsky et al., *New parton distribution functions from a global analysis of quantum chromodynamics*, *Phys. Rev. D* **93** (2016) 033006 [1506.07443].

[30] K.J. Golec-Biernat and M. Wusthoff, *Saturation in diffractive deep inelastic scattering*, *Phys. Rev. D* **60** (1999) 114023 [hep-ph/9903358].

[31] A. Accardi et al., *Electron Ion Collider: The Next QCD Frontier: Understanding the glue that binds us all*, *Eur. Phys. J. A* **52** (2016) 268 [1212.1701].